Covalent adaptable networks through dynamic *N,S*-acetal chemistry: toward recyclable CO_2-based thermosets

Thomas Habets[1], Guillem Seychal[2,3], Marco Caliari[1,3], Jean-Marie Raquez[2], Haritz Sardon[3], Bruno Grignard[1,4], Christophe Detrembleur[1]*

[1] Center for Education and Research on Macromolecules (CERM), CESAM Research Unit, University of Liege, Sart-Tilman B6a, 4000 Liege, Belgium
[2] Laboratory of Polymeric and Composite Materials, Center of Innovation and Research in Materials and Polymers (CIRMAP), University of Mons UMONS, Place du Parc 20, 7000 Mons, Belgium
[3] POLYMAT, University of the Basque Country UPV/EHU, Joxe Mari Korta Center, Avda. Tolosa 7, 20018 Donostia-San Sebastian, Spain
[4] FRITCO_2T Platform, University of Liege, Sart-Tilman B6a, 4000 Liege, Belgium

Abstract

Designing easily recyclable polymers with customized properties is a key challenge to face up environmental concerns and the growing plastics demand. Here, we report a dynamic chemistry between CO_2-sourced alkylidene oxazolidones and thiols that delivers circular non-isocyanate polyurethane networks embedding *N,S*-acetal bonds. Oxazolidones are synthesized from cheap reagents and carbon dioxide. The polymer structure is tuned by monomer design, translating in a wide panel of mechanical properties, ranging from PDMS-like elastomers (Young's modulus (E) = 2.9 MPa and elongation at break (E_{break}) = 159%) to polystyrene-like rigid plastics (E = 2800 MPa, E_{break} = 2%). The dynamic nature of the *N,S*-acetal bond offers multiple closed- and open-loop recycling options, facilitating repeated thermoset reprocessing into the same material or the production of a different one of distinct properties. The versatility of this chemistry shows great potential for preparing materials (including composites) of tunable properties that can be recycled by multiple scenarios.

Introduction

Plastics are ubiquitous in our daily life on account of their vast panel of applications within most economical sectors. The global plastic use accounted for 460 million tons in 2019 and, following worldwide trends, is expected to triple by 2060[1]. Regrettably, plastic waste became one of the greatest environmental threats causing irreversible damages to many ecosystems on the planet. Replacing them is not a feasible option as there are no viable alternatives so far which can match their outstanding features: low weight, affordability, versatility, and durability. A worldwide effort is devoted to re-think the plastics design through valorization of waste[2,3] or by utilizing biobased and/or CO_2-sourced molecules[4–6] to circumvent fully fossil-based chemistry. However, their recycling must be considered as importantly as their production to tackle environmental concerns[7–10]. Thus, appropriate solutions need to be developed in both the design and the recyclability of these materials.

In the recent years, covalent adaptable networks (CANs) have emerged as a new class of polymers whose properties lie between thermoplastics and thermosets[11–15]. Despite their cross-linked 'fixed' structure, recycling is enabled through exchange reactions between dynamic bonds under a certain trigger, most generally heat[16]. Many works already took advantage of bond dynamicity to reprocess conventionally unrecyclable thermoset materials, notably via smart insertion of dynamic disulfide, boronic ester, acetal or Diels-Alder adducts bonds within the polymer matrix[17–21]. However, the reshaping process is most often limited by the high cross-link density and associated viscosity even at high temperature, restraining their processing to compression molding[22,23]. Most examples of CANs

reprocessed using a larger arsenal of techniques are designed with lower cross-link densities[24] through long oligomeric or polymeric chains within their structure to reach lower viscosities at high temperature[20,25–28].

CANs can be categorized in two main categories depending on their bond exchange mechanism[29]. Associative CANs are characterized by a constant cross-link density during reprocessing as bonds associate before breaking, rendering their fast relaxation challenging. To address this issue, smart molecular engineering through additional functional groups and catalysts[16] was successfully implemented to extrude associative CANs imparted with enough short relaxation times[22]. In contrast, dissociative CANs contain bonds that follow a stepwise elimination and addition mechanism, resulting in a loss of cross-link density as a function of temperature.[30] However, the addition of large amount of catalyst or the insertion of specific groups in the matrix are generally needed to shift enough the equilibrium toward the dissociated state to endow the material with enough low viscosity to be reprocessed like thermoplastics[24,31]. Another challenge associated with CANs is the access to milder reprocessing conditions. Most dynamic networks need long exposures to high temperatures and pressures to be reshaped, typically above 150 °C from some minutes to several hours[30,32–34]. Such harsh conditions might generate unwanted side reactions,[14,32,35–37] resulting in material properties alteration during multiple reshaping cycles. Fast reprocessing of CANs in mild conditions is therefore of key interest to facilitate recycling. Lastly, finding new chemistries of high potential in terms of recyclability, cost, scalability, and tunability toward materials with modular thermo-mechanical properties became a new pillar in the search for a more sustainable and affordable future for plastics.

In the last years, many works were devoted to design sustainable polymers containing degradable acetal linkages[38,39]. Recent contributions related to CANs have also shown that acetals and thioacetal derivatives undergo stress relaxation through bond exchange at elevated temperatures, rendering the acetal chemistry a promising platform for making greener materials[31,40–42].

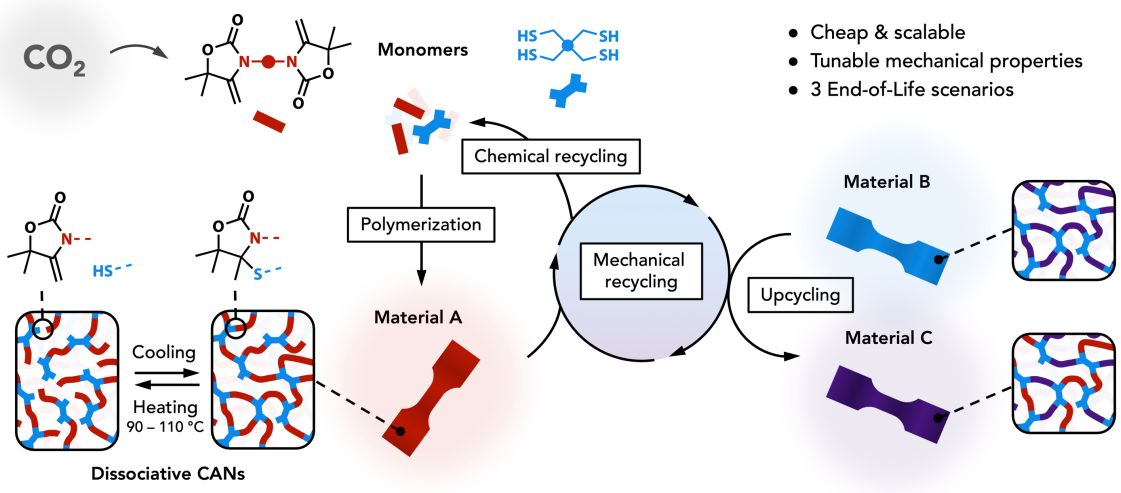

Scheme 1 – Illustration of the alkylidene oxazolidone – thiol chemistry, and overview of the three recycling scenarios of *N,S*-acetal oxazolidone-based dissociative CAN materials (mechanical, chemical and upcycling).

In this work, we introduce a new highly dynamic chemistry based on *N,S*-acetals and its application in CANs. Unlike conventional synthetic approaches, *N,S*-acetals are synthesized by a facile cationic thiol-ene reaction between thiol and exovinylene oxazolidone obtained from CO_2. Their utility is highlighted for the edition and reutilization of thermoset poly(oxazolidone)s, a type of emerging isocyanate-free

polyurethanes with remarkable thermal and chemical stability[43–45]. Mechanistic and kinetic insights of the *N,S*-acetal formation and its dynamicity were first illustrated on model compounds. Then, diverse CO_2-sourced exovinylene bisoxazolidone monomers were prepared and copolymerized with a polythiol at room temperature to provide thermosets featuring a wide diversity of mechanical properties ranging from PDMS-like elastomers to rigid polystyrene-like ones. The *N,S*-oxazolidone bond in the thermosets was proven to be highly dynamic by means of rheology through stress relaxation and temperature sweep cycling experiments. This unique bond dynamicity was then exploited for developing three different recycling scenarios: (i) the facile and rapid mechanical reprocessing by compression molding, extrusion or injection molding of densely cross-linked bulk material, (ii) the closed-loop chemical recycling through depolymerization into the offspring monomers, followed by their repolymerization, and (iii) an upcycling strategy by repurposing two different oxazolidone-based thermosets into a single one with new thermo-mechanical properties (Scheme 1). The utility of this new dynamic chemistry is exemplified by the facile manufacturing of a recyclable structural composite.

Overall, this work provides a new tool for the facile preparation of *N,S*-oxazolidones compounds and recyclable polymer networks from CO_2. To date, there is no example of oxazolidone-based networks with intrinsic recyclability, and recent contributions on poly(oxazolidone)s were focused on linear polymer synthesis[46–50].

Results & Discussion

Inspired by the "click" reaction of enamides with thiols in acidic conditions to provide *N,S*-acetals [51], we aimed to investigate whether the enecarbamate structure within alkylidene oxazolidones **2** exhibits similar reactivity (Figure 1a). Our group has previously confirmed the viability of this chemistry for post-functionalizing linear polymers containing alkylidene oxazolidone moieties[49]. However, a comprehensive understanding of the reaction at the molecular level remains unexplored. Intrigued by the potential of this reaction to deliver novel *N,S*-acetal oxazolidone scaffolds and the presumed dynamic nature of the *N,S*-acetal bond, we conducted initial studies at the model molecule level before implementing this chemistry to macromolecular engineering.

Model reactions

Alkylidene oxazolidones **2** can be obtained via the spontaneous and quantitative reaction between primary amines and CO_2-sourced α-alkylidene cyclic carbonates **αCC**. This reaction yields hydroxyoxazolidones **1**, which are subsequently dehydrated into the desired alkylidene oxazolidones **2** (Figure 1a). Previous works have introduced this last step[48,52], but existing approaches led to a mixture of **1** and **2**. To address this limitation, we developed a novel optimized protocol for the synthesis of **2** at high yields, ensuring both quantitative reaction and potential scalability.

In the frame of this study, we started from a cheap and abundantly available propargyl alcohol, 2-methylbut-3-yn-2-ol, that produced the corresponding α-alkylidene cyclic carbonate **αCC** by the room temperature reaction with CO_2 in the presence of a low catalyst loading (Ag_2CO_3/PPh_3; 1 mol%). After 14 h of reaction at 40 bar, 126 g of **αCC** was obtained in a single batch with a high isolated yield (76 %). The quantitative dehydration of **1** was then realized with methanesulfonic acid (MSA, 0.1 eq.) in refluxing continuously dried acetonitrile (Figure S1), and **2** was collected with a high isolated yield of 77-83% after purification. For the purpose of this work, two compounds were easily produced from two structurally different primary amines, i.e. propylamine (product **2a**) and benzylamine (product **2b**) (Figure 1b).

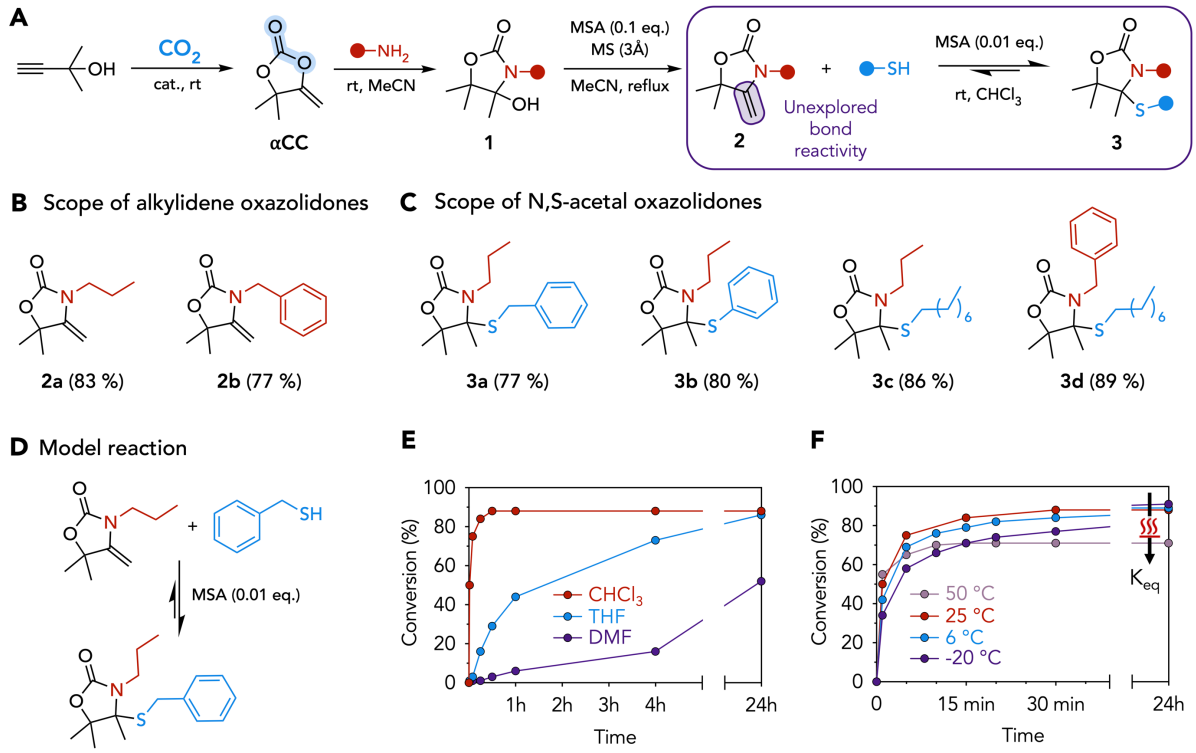

Figure 1 – Overview of the synthetic pathway toward *N,S*-acetal oxazolidones and model reactions. (A) Carboxylation of 2-methylbut-3-yn-2-ol into reactive **αCC**, followed by its aminolysis into hydroxyoxazolidone **1**. Dehydration can be triggered to yield alkylidene oxazolidone **2**. N,S-acetal oxazolidones **3** are then obtained by the cationic addition of the thiol onto **2**. (B) Scope of synthesized alkylidene oxazolidones **2** and (C) *N,S*-acetal oxazolidones **3** (isolated yields in brackets). (D) Model reaction between **2a** and benzyl mercaptan to study the effect of (E) solvent and (F) temperature on the reaction kinetics.

With compounds **2** in our hands, we initiated our investigation by subjecting them to reaction with equimolar contents of thiols to yield *N,S*-acetal oxazolidones **3**. To assess how solvent and temperature influenced the reaction, we conducted reaction kinetics using the model oxazolidone **2a** and a commercial thiol, benzyl mercaptan, in the presence of MSA as acid catalyst (0.01 eq. compared to the oxazolidone), which has shown to efficiently catalyze the cationic thiol-ene reaction[51] (Figure 1d, Figures S21-S24).

Chloroform was the ideal solvent for the reaction, which ended after nearly 15 minutes with the formation of **3a** (Figure 1e). Importantly, the reaction never reached completion and a conversion of 88 % at equilibrium was obtained at 25 °C, in contrast to previously studied enamides which quantitatively provided the product[51]. Solvents with a higher Lewis base character[53] significantly decreased the reaction rate. In THF, a similar conversion required over 4h of reaction and, in DMF, the rection remained uncomplete after two days. Our findings indicate that solvents with a higher base nature tend to act as proton traps, affecting the alkylidene protonation efficiency, in accordance with the previous work of Kloxin et al[51].

Conversions were lower at higher temperature as the dissociated state was entropically favored (71 % at 50 °C) but were slightly increased at a lower temperature (89 % at 6 °C and 91 % at -20 °C) at the cost of longer reaction times (Figure 1f). This suggested that the conversion was dictated by the thermodynamic equilibrium between the associated and the dissociated state, the equilibrium constant being affected by temperature changes.

We probed the reactivity of **2a** with various thiols, i.e. octanethiol, benzyl mercaptan and thiophenol (Figure S25a). Octanethiol behaved similarly to benzyl mercaptan, with a slight increase of the reaction rate, certainly due to a decrease in steric hindrance around the thiol group. Thiophenol reacted rapidly, however its conversion remained low at equilibrium (73 %). Using the more hindered oxazolidone **2b** with octanethiol did not seem to significantly affect the reaction rate (Figure S25b).

The potential of this reaction can be leveraged by choosing ideal conditions (25 °C, excess of thiol) to synthesize novel *N,S*-acetal oxazolidone compounds **3a-d** (Figure 1c) with high isolated yields (up to 89 %). The full characterization of these molecules by NMR spectroscopy and HRMS can be found in Supporting Information (Figures S10-S17). This chemistry therefore opens an avenue to the facile construction of a vast library of compounds whose oxazolidone motifs are of high interest in many fields of chemistry (pharmacology, agriculture, synthetic intermediates, etc.).[54–57]

To have a better insight on the mechanism of this reaction, we performed density functional theory (DFT) calculations at the ωB97-XD/6-311++G(d,p) level of theory with a CPCM solvation model (ε=4.7113, chloroform) (Figure 2a). For simplicity's sake, the system was modelled with methyl groups as substituents for the N and S atoms, mimicking aliphatic chains used in the experimental model reactions. As it might have a drastic impact on calculations, MSA was used as catalyst in the system. Our results revealed that the reaction is performed in two separate steps. The starting reactants complex is very stable compared to separate reactants with a stabilization energy of 13.1 kcal·mol^{-1}. This is enabled by hydrogen bonding interactions between the different species and more especially due to the acidic proton of MSA in interaction with the negatively charged atom of the alkene (Figure S20). This interaction creates a high degree of delocalization in the oxazolidone ring thanks to the presence of the electron-rich nitrogen group in the vicinity of both the alkene and the carbonyl groups. The first step of the reaction, which is the rate-determining step (RDS) of the forward reaction, has a low activation barrier of 7.5 kcal·mol^{-1} explaining the experimentally observed high reaction rate. In this first step, the acidic proton of MSA is transferred to the terminal side of the alkene to form a stabilized carbocation, which is of very similar energy than the reactants complex **int1** (difference of 0.1 kcal·mol^{-1}). The high stabilization of this intermediate **int2** can be explained by the formation of a new stable pi bond between the nitrogen and the carbocation, resulting in a decrease of bond length from 1.373 to 1.292 Å (- 0.081 Å). The N-C(O) bond readily increases its length of 0.073 Å as the nitrogen atom shares less electrons with the carbonyl group (Table S1). In a second time, the thiol adds onto the electrophilic carbon of the ring with a very low barrier of 5.0 kcal·mol^{-1}, thus breaking the pi bond created in the first step. In a concerted manner, the hydrogen of the thiol already in interaction with the catalyst is then completely transferred to form a stabilized complex of the product and the regenerated MSA **int3**, whose energy is -26.3 kcal·mol^{-1}. This enhanced product stability renders the reverse reaction less energetically favorable though the reverse barrier stays rather low with an activation energy of 18.5 kcal·mol^{-1}. These differences in energy support why the equilibrium was shifted towards the product under ambient reaction conditions, with only slight reversibility occurring at room temperature.

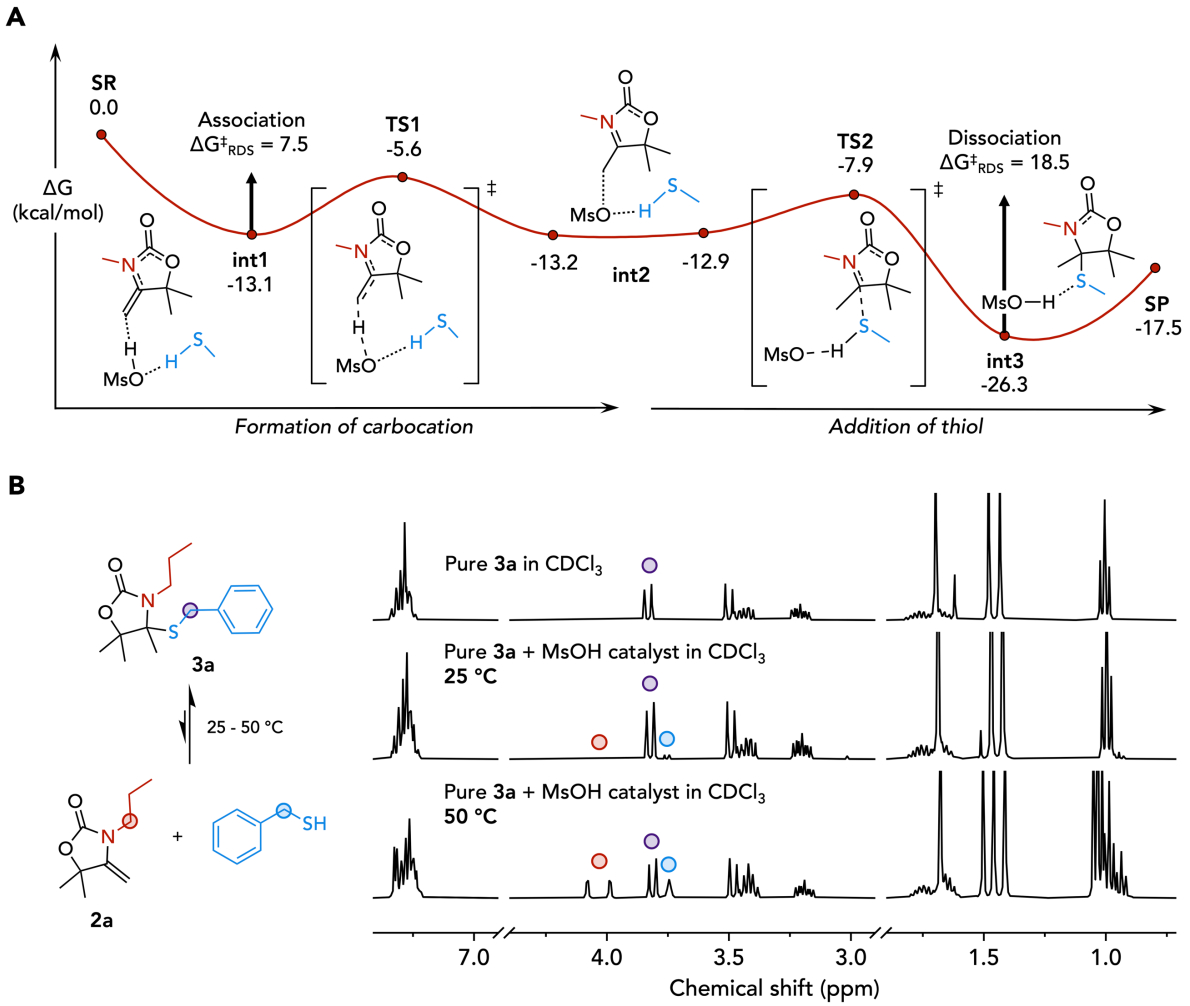

Figure 2 – Energetics of the reaction pathway modelled by DFT and dissociative nature of the *N,S*-acetal oxazolidone moiety. (A) Gibbs-Free Energy profile with intermediates and transition states structures for the reaction of a model alkylidene oxazolidone with a model thiol. Vertical arrows indicate the energy barriers for both the association and the dissociation reactions at their rate-determining step (RDS). (B) Dissociation experiment of **3a** in the presence of MSA in deuterated chloroform ($CDCl_3$) analyzed by ^{1}H-NMR spectroscopy at different temperatures.

To further support that dissociation occurred under ambient conditions, to pure oxazolidone 3a was added by MSA (0.01 eq.) in $CDCl_3$ and the mixture was analyzed by ^{1}H-NMR spectroscopy (Figure 2b). Besides *N,S*-acetal oxazolidone 3a, we observed the formation of the alkylidene oxazolidone 2a and the thiol in low amounts (≈ 3 mol%). Without MSA, only compound 3a was observed. This result provided strong evidence that dissociation slightly occurred in the presence of MSA at room temperature. When increasing the temperature to 50 °C, a great effect on dissociation was observed with the formation of 2a and the thiol in large amount (≈ 25 mol%).

The exchange kinetics was monitored at different temperatures using ^{1}H-NMR spectroscopy by reacting 3a with a fivefold excess of octanethiol in the presence of MSA (0.01 eq. *vs* 3a) (Figures 3a, S26). The reaction was monitored from 20 to 50 °C, showing slow exchange kinetics at 20 °C and strong acceleration of the reaction rate constant k at 50 °C, passing from 2.7×10^{-3} to 23×10^{-3} s^{-1}. The exchange reaction therefore showed a great temperature dependance. An Arrhenius plot was built from the different reaction rate constants k at different temperatures and an activation energy of 14.6 kcal.mol^{-1} was extracted for the bond exchange (Figure 3b-c), lying in the same range of *S,S*-acetal or vinylogous

urethane bonds[42,58] (Table S2). This energy is also of same order as the dissociation energy determined by DFT (18.5 kcal.mol^{-1}). It must be noted that even in the presence of a high excess of thiol, the alkylidene oxazolidone 2a could still be observed in traces amount by NMR during the reaction kinetics, further proving the dissociative mechanism (Figure S26). Overall, the alkylidene oxazolidone – thiol dynamic chemistry showed activity at room temperature with strong increase in bond dynamicity when the temperature was increased, highlighting a high reversible character in mild conditions.

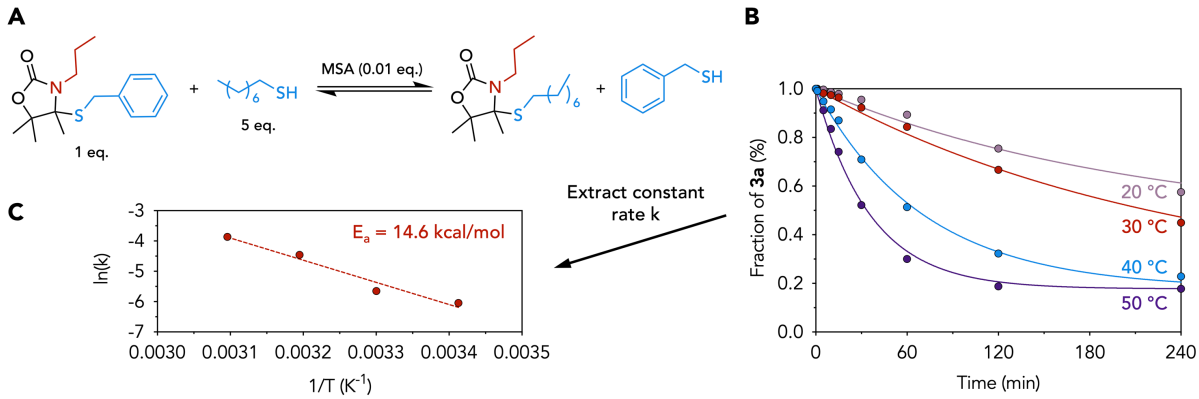

Figure 3 – Exchange reaction kinetics at the model compound level. (A) Model reaction for the exchange kinetic study. (B) Kinetics of exchange at several temperatures (from 20 to 50 °C). (C) Arrhenius plot from the extracted reaction rate constants at the different temperatures of reaction.

Thermoset preparation and characterization

Taking advantage of the highly reversible character of this reaction, we explored its potential for the design of covalent adaptable networks based on *N,S*-acetal bonds. We exploited the versatile and facile α-alkylidene cyclic carbonate chemistry to design bifunctional alkylidene oxazolidone monomers of different structures (Figure 4a). Four compounds **2c-2f** were synthesized from different commercially available diamines: m-xylylenediamine (XDA), 2,2′-(Ethylenedioxy)bis(ethylamine) (DMDO), hexamethylenediamine (HMDA) and Priamine 1075 (PRI). This scope of diamines was chosen to access structurally diverse monomers, which are expected to impart networks with diamine-dependent properties. The synthesis of all four monomers was achieved by reacting CO_2-sourced **αCC** with a diamine in acetonitrile at r.T. Then, tandem dehydration was triggered without isolation of the bis(hydroxyoxazolidone) intermediate using the previously described dehydration setup. All substrates were easily purified by a chromatography-free process in high isolated yield (up to 84 %), rendering their synthesis facile, cheap, and up-scalable (see supporting information for details).

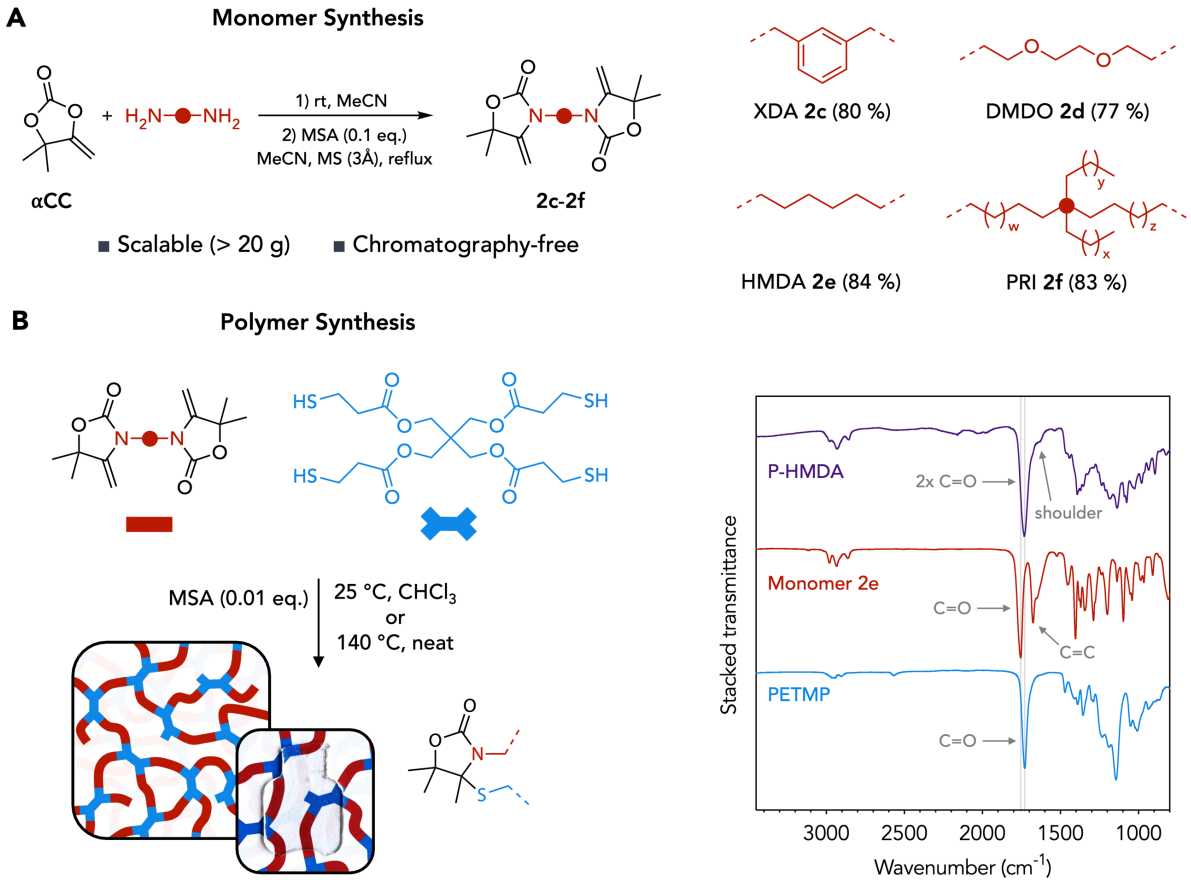

Figure 4 – Monomer and polymer syntheses**.** (A) Tandem synthesis of bis(alkylidene oxazolidone)s **2c-2f** from **αCC** and diamines (isolated yields in brackets). (B) Polymerization of a bis(alkylidene oxazolidone) with PETMP into a cross-linked material. A specimen of P-XDA is displayed to highlight its high transparency. ATR-IR spectra of P-HMDA and its respective monomers.

Different polymers were designed from the oxazolidone monomers 2c-f and a 4-arm thiol, pentaerythritol tetrakis(3-mercaptopropionate) (PETMP) (Figure 4b). For all these syntheses, an equimolar ratio between the oxazolidone and the thiol functions was used, and the reactions were catalyzed by MSA (0.01 eq. *vs* oxazolidone monomer). The polymerization proceeded either in solution or in bulk (Figure S28). When achieved in solution, the mixture of the monomers in chloroform (2 M concentration of reactive functions) was stirred at r.T. until the formation of a gel (between 10 and 60 minutes depending on the monomer). The gel was then recovered and dried under vacuum at 70 °C followed by slow cooling to yield the pure material. Another option, which might be more easily adopted for large-scale production, was the bulk polymerization by stirring the components in the melt at 140 °C for 5 minutes followed by slow cooling to directly yield the pure material. In the two processes, the polymer networks were transparent with a special emphasis for P-XDA showing no coloration (Figure 4b).

Successful polymerization was confirmed via infrared (FT-IR) spectroscopy (Figure 4b). The networks were characterized by an intense elongation at 1732 cm^{-1} contributing for the stretching of the carbonyl groups of both the oxazolidone and ester groups. A very low intensity signal around 1620 cm^{-1} was indicative of some residual alkylidene function (Figures S29-30). This is in line with the previous model reaction study that revealed a non-quantitative conversion of the reactants. Nevertheless, high gel contents were obtained for all polymers in THF (from 87 to 99 %), attesting for the crosslinked nature

of the materials (Table 1). A good swelling (between 140 and 314%) was observed for all polymers in THF (Table 1).

The thermal properties of the polymers were then studied by thermogravimetric analysis (TGA) and differential scanning calorimetry (DSC) (Table 1). All polymers displayed a temperature at 10 % of degradation ($T_{deg,10\%}$) around 300 °C except for P-PRI characterized by a higher value of 366 °C. The highest T_g was recorded for the aromatic P-XDA (T_g = 60 °C) with a more rigid backbone. On the other side, P-PRI picturing more chain mobility was characterized by the lowest T_g (8 °C). P-DMDO and P-HMDA had intermediate T_gs of 51 and 44 °C, respectively.

To extend the scope of materials and modulate their thermo-mechanical properties, four additional polymers were synthesized by mixing pre-defined ratios of XDA or HMDA with PRI. The new polymers were labeled P-(A X)-(B Y) to denote their content in X wt% of monomer A and Y wt% of monomer B. Their temperature of degradation was quite similar, around 300 °C. We expected intermediate T_g for these polymers. Surprisingly, P(HMDA75)-(PRI25) was characterized by the same T_g as P-HMDA (44 °C), and P(XDA75)-(PRI25) was characterized by a similar T_g as P-XDA (62 °C and 60 °C, respectively). By increasing the PRI content to 50 wt% within the materials, their T_g dropped while remaining around 40 °C. Overall, the thermal properties of the networks were judiciously adjusted through the choice of the diamine chemical structure.

Table 1. Thermal properties, swelling ratios, gel contents and mechanical properties of the polymers.

Polymer	$T_{deg,10\%}$[a] (%)	T_g[b] (°C)	SR_{THF}[c] (%)	GC_{THF}[d] (%)	Mechanical properties[e]			
					Young modulus (MPa)	Yield Strength (MPa)	Stress at break (MPa)	Strain at break (%)
P-XDA	296	60	196 ± 6	90.4 ± 0.6	--	--	--	--
P-DMDO	303	51	140 ± 4	99.0 ± 0.3	2806 ± 105	49.5 ± 4.4	49.5 ± 4.4	2.2 ± 0.2
P-HMDA	282	44	215 ± 5	94.8 ± 0.4	1778 ± 116	12.6 ± 1.4	12.6 ± 1.4	0.7 ± 0.1
P-PRI	366	8	287 ± 21	86.6 ± 1.3	2.9 ± 0.1	2.2 ± 0.1	2.2 ± 0.1	159 ± 4
P-(HMDA75)-(PRI25)	289	44	228 ± 1	93.8 ± 0.2	1851 ± 41	34.0 ± 1.2	34.0 ± 1.2	2.1 ± 0.1
P-(HMDA50)-(PRI50)	291	37	205 ± 6	91.2 ± 0.2	655 ± 72	8.6 ± 0.3	13.0 ± 0.3	81 ± 0.3
P-(XDA75)-(PRI25)	289	62	314 ± 6	86.1 ± 0.1	--	--	--	--
P-(XDA50)-(PRI50)	310	43	292 ± 12	93.7 ± 0.4	1238 ± 45	29.9 ± 1.0	20.8 ± 0.8	10 ± 1

[a]Temperature at 10% of degradation determined by TGA.

[b]Glass transition temperature determined from the reversing curve of the first heating rate by modulated DSC.

[c]Swelling ratio (SR) after immersion of the polymer for 24h in solvent (THF).

[d]Gel content (GC) after immersion of the polymer for 24h in solvent (THF).

[e]Mechanical properties evaluated by tensile tests.

Next, the mechanical properties of the various polyoxazolidones thermosets were determined through tensile tests on specimens obtained by compression molding of the samples (Figure 5a). Unfortunately, P-XDA and P-(XDA75)-(PRI25) samples could not be tested due to their extreme brittleness. P-HMDA was a brittle material too, breaking at very low strain (0.7 %). Despite its similar T_g lying between P-XDA and P-HMDA, P-DMDO showed excellent mechanical properties with a Young modulus of 2800 MPa and a yield strength of 50 MPa, with a brittle fracture occurring at low strain (2.2 %). The extra toughness of this polymer compared to P-HMDA was attributed to the higher degree of mobility provided by the presence of the ether bonds within the polymer microstructure. On the other hand, P-PRI demonstrated elastomeric behavior, with a relatively low modulus of 2.9 MPa and an elongation at break of 159%. Interestingly, when PRI was added to the formulation of brittle P-XDA and P-HMDA, the resulting polymer's mechanical behavior was significantly altered. Specifically, P-(HMDA75)-(PRI25) exhibited a modulus of 1850 MPa and a brittle fracture, while increasing the PRI content in P(HMDA50)-(PRI50) decreased the modulus to 655 MPa and resulted in high plastic deformation with an elongation at break of 81%. P(XDA50)-(PRI50) exhibited a modulus of 1240 MPa and plastic deformation.

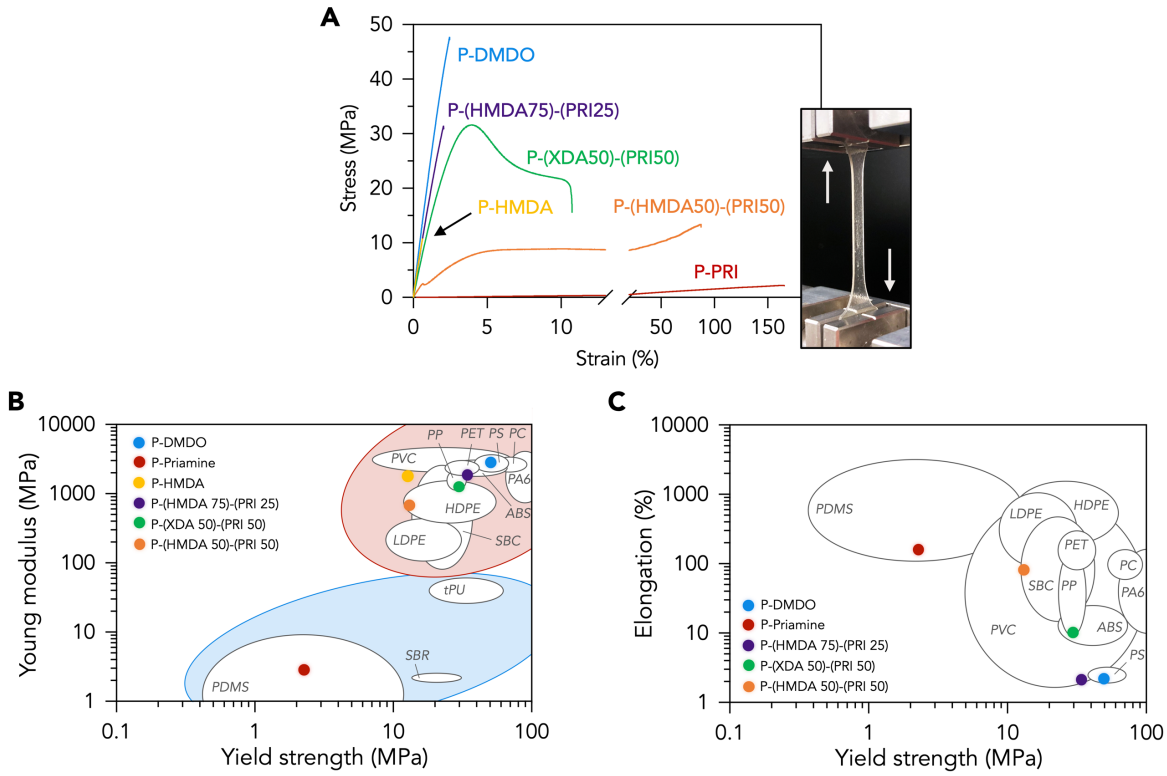

Figure 5 – Mechanical properties of the polymers determined by tensile tests and comparison to commodity polymers**.** (A) Stress – strain curves of all polymers displaying a large range of properties. (B) Ashby plot showing Young modulus and yield strength compared to commodity polymers. (C) Similar Ashby plot showing elongation and yield strength. Commodity polymers mechanical properties were found in the literature[59].

To compare the properties of the synthesized polymers to commodity polymers, we plotted Ashby diagrams[60] based on three critical parameters: the Young's modulus, the yield strength, and the elongation at break (Figure 5b-c). These plots revealed a wide diversity in the mechanical properties of the synthesized polymers, with some of them exhibiting properties comparable to some commodity

polymers. For example, P-DMDO had similar properties to polystyrene (PS), with a modulus, strength, and elongation within the literature values. Furthermore, P-PRI was located in the PDMS area of the diagram, while P(XDA50)-(PRI50) was situated in the polypropylene (PP) zone, albeit with low elongation. Despite P(HMDA75)-(PRI25) and P(HMDA50)-(PRI50) exhibiting intriguing properties, they did not meet those of the reported commodity polymers.

These results illustrate the huge potential of our new polymers to furnish materials of tunable mechanical properties by simply adapting the alkylidene oxazolidone monomer structure. Moreover, this study only represents a limited overview of the myriad of possibilities through monomer design and formulation to develop a wide range of materials with on-demand modular properties to fit with the specification of diverse applications.

Dynamic behavior of the networks

The dynamic behavior of the networks was then characterized by rheology and exemplified for P-HMDA in Figure 6. First, the temperature-dependence on the storage (G') and loss modulus (G'') was assessed by a temperature sweep experiment (Figure 6a). Values below T_g could not be determined by rheology as the sample was hard, resulting in a poor surface contact between the rheometer plateau and the specimen[61]. Above T_g, the sample showed a higher value of G' than G'', indicating that the material was in a cross-linked rubber state. Importantly, G' showed a constant decreasing trend, attesting for the progressive loss of cross-linking density with increasing temperature. This result was in line with the dissociative nature of the bonds as observed in the model compounds study. The curves tend to cross above 80 °C where enough dissociation occurred to de-crosslink the material and enable flow. The crossover point between the two curves represents the gel-to-sol transition and was denoted $T_{gel\text{-}to\text{-}sol}$ for the different polymers (Table 2).

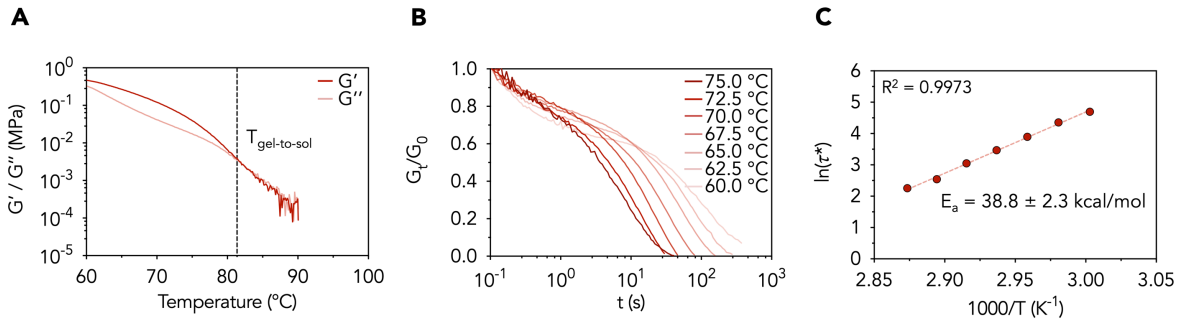

Figure 6 – Rheological experiments conducted on P-HMDA**.** (A) Temperature sweep. (B) Stress relaxation at different temperatures whose extracted characteristic relaxation times could fit the (C) Arrhenius law to obtain an energy of activation.

Table 2. Gel-to-sol transition and flow activation energy for the polymers studied by rheology.

Polymer	$T_{gel\text{-}to\text{-}sol}$[a] (°C)	E_{flow}[b] (kcal·mol^{-1})
P-XDA	--[c]	--[c]
P-DMDO	91.3	26.4 ± 3.0
P-HMDA	81.4	38.8 ± 2.3
P-PRI	72.6	34.5 ± 2.8

[a] Gel-to-sol transition temperature as determined by temperature sweep rheology.

[b] Flow activation energy (E_{flow}) as determined by stress relaxation measurements in rheology.

[c] Could not be determined.

Similar trends were observed for P-DMDO and P-PRI, each of them showing different $T_{gel\text{-}to\text{-}sol}$ transition temperatures (Figure S39-S41). P-DMDO presented a higher transition of 91 °C and P-PRI a lower one of 73 °C. As P-PRI was characterized by a low T_g, rheological data were recorded from room temperature. Interestingly, the value of G' was slowly decreasing from 30 to 55 °C, indicating a slight loss of cross-link density at low temperature. An abrupt drop was observed starting around 60 °C until the gel-to-sol transition at 72.6 °C.

Stress-relaxation experiments were achieved before the flow transition threshold in the viscoelastic region of the networks. As observed in Figure 6b for P-HMDA, the material readily relaxed the applied stress through bond dynamicity. The normalized stress relaxation curves have shown to follow a three-element Maxwell model, revealing the presence of three distinct relaxation modes during the material topology reorganization. However, most studies on CANs revealed that single-element Maxwell or stretched exponential models were generally accurately fitting the relaxation experiments data[12]. On the other side, multi-element Maxwell could be effectively used to describe materials with kinetically different exchange processes[62,63]. At each temperature were extracted three characteristic relaxation times (τ_1, τ_2 and τ_3). τ_1 and τ_2 showed to be independent from temperature changes and were both of relatively short timescale (0.1-0.7 s for τ_1 and 0.7-15 s for τ_2) (Figures S39-S41; Table S3). Thus, we hypothesized these relaxation modes to be attributed to chain rearrangement at stress exposition[64]. Although these two first relaxation modes with short timescales may not interfere in the network reprocessability, the use of a three-element Maxwell model is critical to correctly fit and extract reliable data. The last relaxation mode of characteristic relaxation time τ_3 was characterized by a strong temperature dependence and may be attributed to bond dynamicity within the network. The different characteristic relaxation times τ_3 were plotted against temperature in a typical Arrhenius plot and an excellent linear correlation was observed, thus enabling the determination of a flow energy activation $E_{a,flow}$ of 38.8 kcal·mol^{-1} (Figure 6c). Stress relaxation experiments on P-DMDO and P-PRI showed that the polymer matrix and thereby, the monomer structure, had a strong influence on the viscoelastic behavior of the polymer (Table 2). P-DMDO was characterized by a lower $E_{a,flow}$ of 26.4 kcal·mol^{-1}, indicating a less pronounced sensitivity of the viscosity to temperature[14,65]. P-DMDO was indeed imparted with a shorter relaxation time τ_3 at 60 °C (88 s) but higher at 75 °C (15 s). This result was in line with the temperature sweep experiment displaying a higher $T_{gel\text{-}to\text{-}sol}$ transition for P-DMDO than P-HMDA despite their close T_g. On the other side, P-PRI was characterized by a lower but yet similar $E_{a,flow}$ as P-HMDA, of 34.5 kcal·mol^{-1}. The early gel-to-sol transition observed in P-PRI was rationalized by an increased chain mobility. However, matrix effects on CANs are yet still not fully understood and many parameters are thought to play a role such as polarity changes[64], solvation effects, cross-linking density and degree of chain flexibility[66]. Overall, monomer structure seems to have critical influence on the viscoelastic properties of *N,S*-acetal oxazolidone dynamic networks and a better rationalization of the experimental results might be needed to further understand all the structural effects. This study is however out of scope of this paper. The determined flow energy activation for the different studied polymers are in the same range of reported *S,S*-thioacetal dynamic networks reported by the group of Du Prez[42] (Table S2).

Overall, this rheological study suggests a high reprocessing ability for these materials which are able to relax extremely rapidly (relaxation times in the order of seconds) in their rubber state and can even flow as thermoplastics above their gel-to-sol transition temperature where the cross-linking integrity is lost.

Recycling of the networks

While most studies on CANs materials mainly display one or two recycling routes, this work exploited the highly reversible character of the alkylidene oxazolidone-thiol chemistry to provide three different end-of-life scenarios for the materials (Scheme 2). Multiplying the recycling possibilities for new

emerging plastics is of great interest as the recycling approach might be selected depending on the market needs and the state of the material after use.

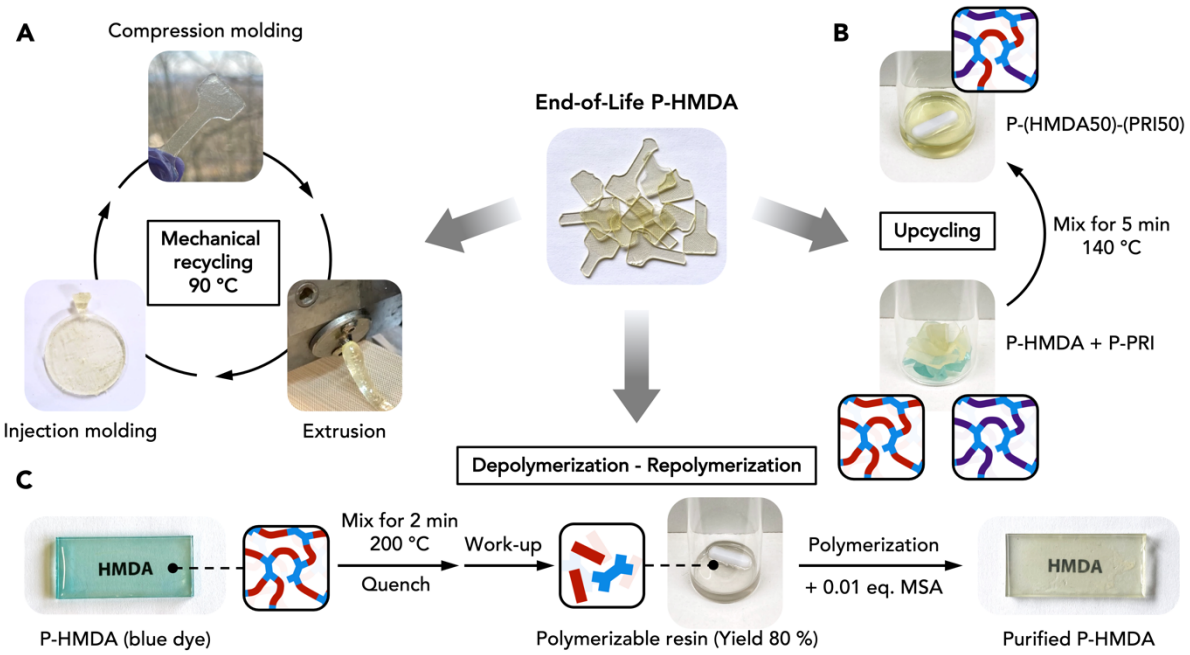

Scheme 2 – End-of-life scenarios for P-HMDA. (A) Mechanical recycling using compression molding, extrusion, and injection molding. (B) Upcycling of P-HMDA and P-PRI toward P-(HMDA50)-(PRI50). (C) Chemical recycling through depolymerization and re-polymerization of contaminated P-HMDA.

Mechanical recycling

The most straightforward approach is the mechanical recycling (Scheme 2a). Although conventional networks cannot be reshaped, stress can be dissipated in CANs by virtue of bond dynamicity and reshaping is therefore made possible. As highlighted by rheological investigations, the polymers reached very low complex viscosities η^* (in the range of 10 to 40 Pa·s at 90 °C) (Figure S42) and flowed at temperatures above the gel-to-sol transition. With this in mind, we first reprocessed P-HMDA by compression molding at 90 °C (in the flowing state) for 10 min under mild pressure (1 ton metric). Upon cooling, the material was recovered from the molds. We also successfully subjected P-HMDA to extrusion at high rate (150 rpm) or injection molding at 90 °C. Reshaping the network was thus possible through multiple industrially relevant techniques in mild conditions and in a short timeframe while most studied CANs require long exposition to high pressure and/or temperature[30,32–34]. In all cases, T_g as well as IR spectrum of the reprocessed polymer were identical to the starting material, suggesting no degradation (Figure S43).

We performed on-line storage modulus measurement as a function of time and temperature over up to 10 cycles (Figure 7). The sample, heated from 60 to 90 °C and cooled down to 60 °C at each cycle, displayed total recovery of the storage modulus. It must be noted that after cooling at 1 °C/min, around 85 % of the storage modulus was recovered. Additional 10 minutes at 60 °C allowed for a total recovery of G' before beginning a new cycle, highlighting that slow cooling was critical to recover the starting material properties. This experiment evidenced that the network underwent total disassembly to a flowing state at 90 °C by cycling above and below the gel-to-sol transition temperature with a total and reproducible recovery of the storage modulus, i.e. of the cross-link density within the material, without any hysteresis. This suggested that these materials might undergo a significant number of fast reprocessing cycles at mild temperatures, well below the degradation of the polymer, thus avoiding

material degradation that might happen in CANs exposed to high pressure and temperatures for a prolonged period of time[14].

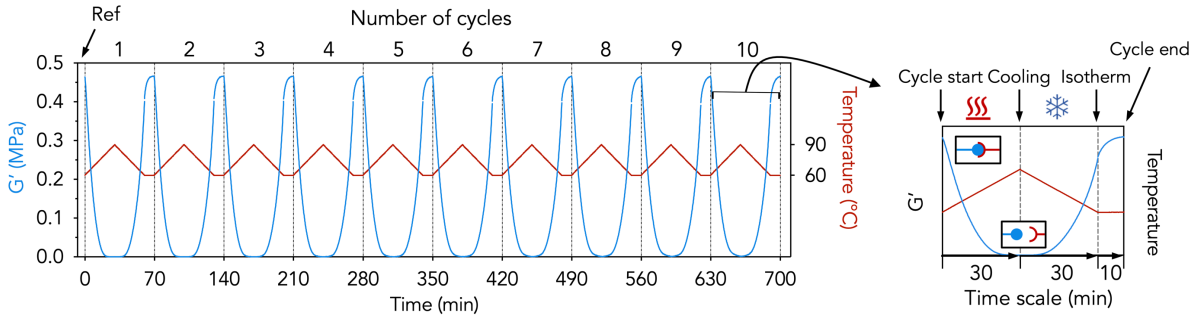

Figure 7 – Temperature sweep cycling test on P-HMDA. For P-HMDA, a temperature sweep cycling test was performed at heating and cooling rates of 1 °C/min between 60 and 90 °C. The storage modulus G' was totally recovered at the end of each cycle.

Upcycling

Recently, it was demonstrated that upcycling of CANs was possible through bond exchange between two distinct materials into a divergent one[67,68]. Dichtel et al. notably demonstrated that two soft and hard polyurethane networks could be mixed enough efficiently to provide a new material by extrusion at 200 °C. An akin strategy can be used in our case by mixing two different *N,S*-acetal oxazolidone dissociative CANs. Upon thermal treatment above the gel-to-sol transition, bond rupture enabled the material to flow, delivering back alkylidene oxazolidone and thiol functionalities and, upon cooling, random re-association of the bonds was expected to provide a hybrid network consisting of mixed structures (Scheme 2b). This was illustrated by efficiently mixing identical contents of two different materials, P-HMDA and P-PRI, at 140 °C for 5 min under solvent-free conditions using a magnetic stirrer, and then to slowly cool down the mixture. DSC and IR analyses evidenced identical T_g and IR spectra than the previously synthesized P(HMDA50)-(PRI50), suggesting that the mixture of the two separate networks were converted into the mixed one (Figure S44). This approach enabled to easily upcycle the end-of-life networks into new ones exhibiting distinct properties.

Chemical recycling

The chemical recycling is the third considered end-of-life option (Scheme 2c). This approach, especially the one that considers the depolymerization into the constitutive monomers, is highly desirable as it generally allows to recover the monomers from impurities such as dyes and other additives[8,69].

Acidic hydrolysis of acetal linkages is a common and attractive way to promote degradation and recycling of polymers in mild conditions[31,41,70]. Thus, the presence of the *N,S*-acetal linkages could render poly(oxazolidone)s scaffolds sensitive to acidic aqueous environments. However, *N,S*-acetals derivatives might be more resistant than oxygen-containing *S,O*- and *O,O*-acetals[51]. Low swelling ratios were observed in water after 24h for all synthesized polymers, the highest value being 2% for P-DMDO. Lowering the pH using acidic aqueous solutions of H_2SO_4 at different concentrations (0.1, 1.0 and 5.0 M) did not lead to any degradation with gel contents as high as 99% and IR spectra showed no difference compared to the pristine polymer (Figure S45), attesting for the resistance of the polymers to acidic aqueous environment.

However, the versatility of the *N,S*-acetal oxazolidone chemistry and its high dissociative character at high temperatures allowed us to find another approach toward a recovery of the constitutive monomers. We synthesized P-HMDA containing a blue dye (methylene blue) as a model additive. In order to shift

the equilibrium toward the monomers and thus to favor depolymerization, we heated the network at 200 °C for 2 minutes only. We then quenched the medium with a catalytic amount of triethylamine (3 eq. per equivalent of MSA) to avoid the MSA-catalyzed reverse reaction, quantitatively yielding a mixture of constitutive monomers and quenched catalyst (Figure S46). The mixture was purified by filtration through activated charcoal to remove the dye followed by a simple liquid extraction with water to remove triethylamine and MSA. After evaporation of the solvent, a colorless viscous resin was obtained. ^{1}H-NMR analysis of the resin revealed the presence of the two starting monomers in equimolar amount that were recovered at 80 % yield (Figure S46). By adding MSA to this mixture and following the synthetic procedure, P-HMDA was recovered with identical DSC and IR results as the starting product (Figure S47).

Composite preparation and recycling

Thermosets are largely used in composites to furnish high performance light structural materials used for instance in wind turbine blades, aeronautics, automotive, etc.[71] However, the recycling of composites is an important issue due to the difficulty to separate the filler from the crosslinked polymer matrix. For the proof of concept to illustrate the potential of our technology in composite preparation and in their facile recycling, we prepared a composite composed of flax as the filler and P-DMDO as the network matrix. For that purpose, P-DMDO was hot pressed on flax under 3 bars of pressure at 100 °C for 15 minutes (Figure 8). This straightforward process was aided by the very low viscosity of the polymer above its gel-to-sol transition temperature, rendering the filler impregnation a facile task. As expected, the composite tensile strength was strongly increased compared to the lone polymer (170 *vs* 50 MPa) as well as the Young modulus (5700 *vs* 2800 MPa) (Figure 8). The strain at break passed from 2.2 % to 3.5 %.

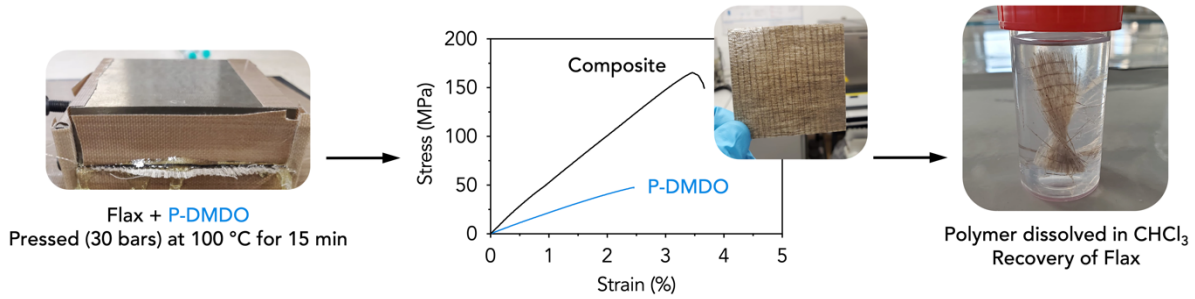

Figure 8 – Composite preparation from flax and P-DMDO. Grinded P-DMDO was pressed with Flax to provide a composite material with excellent mechanical properties. Polymer-free flax could be recovered by dissociation of the polymer matrix in $CHCl_3$.

To separate the fibers from the crosslinked matrix, we exploited the dynamicity of the *N,S*-acetal type oxazolidone linkages. Based on our model reaction reported in Figure 2b, the *N,S*-acetal linkages slowly dissociated in chloroform. By immersing the composite in a large volume of chloroform to displace the equilibrium towards the dissociated state, P-DMDO was completely dissolved after one day at room temperature. While dissolution in organic solvent is generally unwanted for polymer networks and composites that should be solvent resistant, *N,S*-acetal based polyoxazolidone networks were only soluble in a large amount of this specific solvent. This allowed the recovery of the filler when needed (Figure S48). Under identical conditions, no dissolution was noted in THF nor DMF, consistently with the model reactions that demonstrated extremely slow kinetics of reaction in these solvents.

Conclusion

In this work, the alkylidene oxazolidone – thiol chemistry that reversibly delivered *N,S*-acetal type oxazolidone scaffolds was studied at the model reaction level, attesting for fast kinetics in mild conditions with a great dynamic character. The synthesis of bifunctional alkylidene oxazolidone monomers was reported to be easy, affordable, and scalable starting from a readily available propargyl alcohol coupled with CO_2 and a primary diamine. Different polymer networks were synthesized from structurally divergent monomers and a commercially available tetrathiol in the presence of a catalytic amount of methane sulfonic acid (MSA). Networks with a wide range of mechanical properties were prepared, ranging from PDMS-like elastomers to rigid polystyrene-like ones. The highly dynamic character of the covalent adaptable networks was highlighted by rheological study reflecting observations made at the model level. High dissociation rates can be accessible in relatively mild conditions, thus enabling fast reprocessing with thermoplastic-like techniques such as extrusion and injection molding without promoting any side reactions and material alteration. Through this high dynamicity, two divergent materials were also mixed and upcycled by fast dissociation and random re-association events to furnish a new scaffold with distinct properties. At high temperatures, total dissociation was obtained in minutes timeframe, yielding back the initial monomers that could be repolymerized into the same network. Lastly, this chemistry showed potential to be easily applied to composite materials with recycling possibilities. Further work will be devoted to diversify thermal and mechanical properties of the networks with the objective to broaden the application field of this very promising family of easily recyclable polymer networks. Overall, this study shows great potential for constructing a wide range of circular materials that might find applications across the numerous domains covered by polyurethanes, and well beyond as the dynamic linkages might be introduced in other thermosets for improved recyclability.

Supporting Information

The Supporting Information is available free of charge.

Author information

Corresponding author

Further information and requests for resources should be directed to and will be fulfilled by the lead contact, Christophe Detrembleur (christophe.detrembleur@uliege.be).

Author contributions

T.H. and C.D. conceived the idea and designed the experiments. T.H. carried out the experiments and the DFT calculations. T.H. and M.C. discussed the results and participated in discussions related to research directions. T.H. and G.S. performed tensile tests. G.S. designed the composite material. T.H., B.G., and C.D. co-wrote the manuscript. T.H., J-M.R., H.S., B.G., and C.D. edited the manuscript. C.D. got the funding and directed the project.

Declaration of interests

The authors declare no competing interests.

Acknowledgments

The authors of Liege thank FNRS for the financial support in the frame of the CO_2Switch project. C.D. is a F.R.S.-FNRS Research Director and J.M.R is a F.R.S.-FNRS Senior Research Associate. Computational resources have been provided by the Consortium des Équipements de Calcul Intensif (CÉCI), funded by the Fonds de la Recherche Scientifique de Belgique (F.R.S.-FNRS) under Grant No. 2.5020.11 and by the Walloon Region. The authors would like to thank the financial support provided by the NIPU-EJD project; part of this project (composite preparation and recycling) has received funding

from the European Union's Horizon 2020 research and innovation program under the Marie Skłodowska-Curie grant agreement No 955700.

References

(1) OECD. *Global Plastics Outlook: Policy Scenarios to 2060*; OECD, 2022. https://doi.org/10.1787/aa1edf33-en.

(2) Grignard, B.; Gennen, S.; Jérôme, C.; Kleij, A. W.; Detrembleur, C. Advances in the Use of CO_2 as a Renewable Feedstock for the Synthesis of Polymers. *Chem. Soc. Rev.* **2019**, *48* (16), 4466–4514. https://doi.org/10.1039/C9CS00047J.

(3) Xu, Y.; Lin, L.; Xiao, M.; Wang, S.; Smith, A. T.; Sun, L.; Meng, Y. Synthesis and Properties of CO2-Based Plastics: Environmentally-Friendly, Energy-Saving and Biomedical Polymeric Materials. *Progress in Polymer Science* **2018**, *80*, 163–182. https://doi.org/10.1016/j.progpolymsci.2018.01.006.

(4) Cywar, R. M.; Rorrer, N. A.; Hoyt, C. B.; Beckham, G. T.; Chen, E. Y.-X. Bio-Based Polymers with Performance-Advantaged Properties. *Nat Rev Mater* **2021**, *7* (2), 83–103. https://doi.org/10.1038/s41578-021-00363-3.

(5) Hayes, G.; Laurel, M.; MacKinnon, D.; Zhao, T.; Houck, H. A.; Becer, C. R. Polymers without Petrochemicals: Sustainable Routes to Conventional Monomers. *Chem. Rev.* **2023**, *123* (5), 2609–2734. https://doi.org/10.1021/acs.chemrev.2c00354.

(6) Zhao, X.-L.; Tian, P.-X.; Li, Y.-D.; Zeng, J.-B. Biobased Covalent Adaptable Networks: Towards Better Sustainability of Thermosets. *Green Chem.* **2022**, *24* (11), 4363–4387. https://doi.org/10.1039/D2GC01325H.

(7) Jehanno, C.; Alty, J. W.; Roosen, M.; De Meester, S.; Dove, A. P.; Chen, E. Y.-X.; Leibfarth, F. A.; Sardon, H. Critical Advances and Future Opportunities in Upcycling Commodity Polymers. *Nature* **2022**, *603* (7903), 803–814. https://doi.org/10.1038/s41586-021-04350-0.

(8) Coates, G. W.; Getzler, Y. D. Y. L. Chemical Recycling to Monomer for an Ideal, Circular Polymer Economy. *Nat Rev Mater* **2020**, *5* (7), 501–516. https://doi.org/10.1038/s41578-020-0190-4.

(9) Kosloski-Oh, S. C.; Wood, Z. A.; Manjarrez, Y.; De Los Rios, J. P.; Fieser, M. E. Catalytic Methods for Chemical Recycling or Upcycling of Commercial Polymers. *Mater. Horiz.* **2021**, *8* (4), 1084–1129. https://doi.org/10.1039/D0MH01286F.

(10) Korley, L. T. J.; Epps, T. H.; Helms, B. A.; Ryan, A. J. Toward Polymer Upcycling—Adding Value and Tackling Circularity. *Science* **2021**, *373* (6550), 66–69. https://doi.org/10.1126/science.abg4503.

(11) Zheng, N.; Xu, Y.; Zhao, Q.; Xie, T. Dynamic Covalent Polymer Networks: A Molecular Platform for Designing Functions beyond Chemical Recycling and Self-Healing. *Chem. Rev.* **2021**, *121* (3), 1716–1745. https://doi.org/10.1021/acs.chemrev.0c00938.

(12) Zhang, V.; Kang, B.; Accardo, J. V.; Kalow, J. A. Structure–Reactivity–Property Relationships in Covalent Adaptable Networks. *J. Am. Chem. Soc.* **2022**, *144* (49), 22358–22377. https://doi.org/10.1021/jacs.2c08104.

(13) Kloxin, C. J.; Bowman, C. N. Covalent Adaptable Networks: Smart, Reconfigurable and Responsive Network Systems. *Chem. Soc. Rev.* **2013**, *42* (17), 7161–7173. https://doi.org/10.1039/C3CS60046G.

(14) Scheutz, G. M.; Lessard, J. J.; Sims, M. B.; Sumerlin, B. S. Adaptable Crosslinks in Polymeric Materials: Resolving the Intersection of Thermoplastics and Thermosets. *J. Am. Chem. Soc.* **2019**, *141* (41), 16181–16196. https://doi.org/10.1021/jacs.9b07922.

(15) Podgórski, M.; Fairbanks, B. D.; Kirkpatrick, B. E.; McBride, M.; Martinez, A.; Dobson, A.; Bongiardina, N. J.; Bowman, C. N. Toward Stimuli-Responsive Dynamic Thermosets through

Continuous Development and Improvements in Covalent Adaptable Networks (CANs). *Adv. Mater.* **2020**, *32* (20), 1906876. https://doi.org/10.1002/adma.201906876.
(16) Montarnal, D.; Capelot, M.; Tournilhac, F.; Leibler, L. Silica-Like Malleable Materials from Permanent Organic Networks. *Science* **2011**, *334* (6058), 965–968. https://doi.org/10.1126/science.1212648.
(17) Clarke, R. W.; Sandmeier, T.; Franklin, K. A.; Reich, D.; Zhang, X.; Vengallur, N.; Patra, T. K.; Tannenbaum, R. J.; Adhikari, S.; Kumar, S. K.; Rovis, T.; Chen, E. Y.-X. Dynamic Crosslinking Compatibilizes Immiscible Mixed Plastics. *Nature* **2023**, *616* (7958), 731–739. https://doi.org/10.1038/s41586-023-05858-3.
(18) Bowman, C. N.; Kloxin, C. J. Covalent Adaptable Networks: Reversible Bond Structures Incorporated in Polymer Networks. *Angew. Chem. Int. Ed.* **2012**, *51* (18), 4272–4274. https://doi.org/10.1002/anie.201200708.
(19) Fortman, D. J.; Brutman, J. P.; De Hoe, G. X.; Snyder, R. L.; Dichtel, W. R.; Hillmyer, M. A. Approaches to Sustainable and Continually Recyclable Cross-Linked Polymers. *ACS Sustainable Chem. Eng.* **2018**, *6* (9), 11145–11159. https://doi.org/10.1021/acssuschemeng.8b02355.
(20) Röttger, M.; Domenech, T.; Van Der Weegen, R.; Breuillac, A.; Nicolaÿ, R.; Leibler, L. High-Performance Vitrimers from Commodity Thermoplastics through Dioxaborolane Metathesis. *Science* **2017**, *356* (6333), 62–65. https://doi.org/10.1126/science.aah5281.
(21) Adzima, B. J.; Aguirre, H. A.; Kloxin, C. J.; Scott, T. F.; Bowman, C. N. Rheological and Chemical Analysis of Reverse Gelation in a Covalently Cross-Linked Diels−Alder Polymer Network. *Macromolecules* **2008**, *41* (23), 9112–9117. https://doi.org/10.1021/ma801863d.
(22) Taplan, C.; Guerre, M.; Winne, J. M.; Du Prez, F. E. Fast Processing of Highly Crosslinked, Low-Viscosity Vitrimers. *Mater. Horiz.* **2020**, *7* (1), 104–110. https://doi.org/10.1039/C9MH01062A.
(23) Bapat, A. P.; Sumerlin, B. S.; Sutti, A. Bulk Network Polymers with Dynamic B–O Bonds: Healable and Reprocessable Materials. *Mater. Horiz.* **2020**, *7* (3), 694–714. https://doi.org/10.1039/C9MH01223K.
(24) Delahaye, M.; Tanini, F.; Holloway, J. O.; Winne, J. M.; Du Prez, F. E. Double Neighbouring Group Participation for Ultrafast Exchange in Phthalate Monoester Networks. *Polym. Chem.* **2020**, *11* (32), 5207–5215. https://doi.org/10.1039/D0PY00681E.
(25) Yang, K.; Grant, J. C.; Lamey, P.; Joshi-Imre, A.; Lund, B. R.; Smaldone, R. A.; Voit, W. Diels–Alder Reversible Thermoset 3D Printing: Isotropic Thermoset Polymers via Fused Filament Fabrication. *Adv. Funct. Mater.* **2017**, *27* (24), 1700318. https://doi.org/10.1002/adfm.201700318.
(26) Cao, Y.; Rong, M. Z.; Zhang, M. Q. Covalent Adaptable Networks Impart Smart Processability to Multifunctional Highly Filled Polymer Composites. *Composites Part A: Applied Science and Manufacturing* **2021**, *151*, 106647. https://doi.org/10.1016/j.compositesa.2021.106647.
(27) Chen, S.; Wang, F.; Peng, Y.; Chen, T.; Wu, Q.; Sun, P. A Single Molecular Diels-Alder Crosslinker for Achieving Recyclable Cross-Linked Polymers. *Macromol. Rapid Commun.* **2015**, *36* (18), 1687–1692. https://doi.org/10.1002/marc.201500257.
(28) Feng, H.; Ma, S.; Xu, X.; Li, Q.; Wang, B.; Lu, N.; Li, P.; Wang, S.; Yu, Z.; Zhu, J. Facile Synthesis of Hemiacetal Ester-Based Dynamic Covalent Polymer Networks Combining Fast Reprocessability and High Performance. *Green Chem.* **2021**, *23* (22), 9061–9070. https://doi.org/10.1039/D1GC02773E.
(29) Winne, J. M.; Leibler, L.; Du Prez, F. E. Dynamic Covalent Chemistry in Polymer Networks: A Mechanistic Perspective. *Polym. Chem.* **2019**, *10* (45), 6091–6108. https://doi.org/10.1039/C9PY01260E.

(30) Elling, B. R.; Dichtel, W. R. Reprocessable Cross-Linked Polymer Networks: Are Associative Exchange Mechanisms Desirable? *ACS Cent. Sci.* **2020**, *6* (9), 1488–1496. https://doi.org/10.1021/acscentsci.0c00567.
(31) Li, Q.; Ma, S.; Li, P.; Wang, B.; Yu, Z.; Feng, H.; Liu, Y.; Zhu, J. Fast Reprocessing of Acetal Covalent Adaptable Networks with High Performance Enabled by Neighboring Group Participation. *Macromolecules* **2021**, *54* (18), 8423–8434. https://doi.org/10.1021/acs.macromol.1c01046.
(32) Fortman, D. J.; Brutman, J. P.; Cramer, C. J.; Hillmyer, M. A.; Dichtel, W. R. Mechanically Activated, Catalyst-Free Polyhydroxyurethane Vitrimers. *J. Am. Chem. Soc.* **2015**, *137* (44), 14019–14022. https://doi.org/10.1021/jacs.5b08084.
(33) Snyder, R. L.; Fortman, D. J.; De Hoe, G. X.; Hillmyer, M. A.; Dichtel, W. R. Reprocessable Acid-Degradable Polycarbonate Vitrimers. *Macromolecules* **2018**, *51* (2), 389–397. https://doi.org/10.1021/acs.macromol.7b02299.
(34) Obadia, M. M.; Mudraboyina, B. P.; Serghei, A.; Montarnal, D.; Drockenmuller, E. Reprocessing and Recycling of Highly Cross-Linked Ion-Conducting Networks through Transalkylation Exchanges of C–N Bonds. *J. Am. Chem. Soc.* **2015**, *137* (18), 6078–6083. https://doi.org/10.1021/jacs.5b02653.
(35) Delahaye, M.; Winne, J. M.; Du Prez, F. E. Internal Catalysis in Covalent Adaptable Networks: Phthalate Monoester Transesterification As a Versatile Dynamic Cross-Linking Chemistry. *J. Am. Chem. Soc.* **2019**, *141* (38), 15277–15287. https://doi.org/10.1021/jacs.9b07269.
(36) Denissen, W.; Winne, J. M.; Du Prez, F. E. Vitrimers: Permanent Organic Networks with Glass-like Fluidity. *Chem. Sci.* **2016**, *7* (1), 30–38. https://doi.org/10.1039/C5SC02223A.
(37) Wang, S.; Ma, S.; Li, Q.; Yuan, W.; Wang, B.; Zhu, J. Robust, Fire-Safe, Monomer-Recovery, Highly Malleable Thermosets from Renewable Bioresources. *Macromolecules* **2018**, *51* (20), 8001–8012. https://doi.org/10.1021/acs.macromol.8b01601.
(38) Abel, B. A.; Snyder, R. L.; Coates, G. W. Chemically Recyclable Thermoplastics from Reversible-Deactivation Polymerization of Cyclic Acetals. *Science* **2021**, *373* (6556), 783–789. https://doi.org/10.1126/science.abh0626.
(39) Shen, T.; Chen, K.; Chen, Y.; Ling, J. Ring-Opening Polymerization of Cyclic Acetals: Strategy for Both Recyclable and Degradable Materials. *Macromol. Rapid Commun.* **2023**, *44* (13), 2300099. https://doi.org/10.1002/marc.202300099.
(40) Kariyawasam, L. S.; Rolsma, J.; Yang, Y. Chemically Recyclable Dithioacetal Polymers via Reversible Entropy-Driven Ring-Opening Polymerization**. *Angew Chem Int Ed* **2023**, *62* (26), e202303039. https://doi.org/10.1002/anie.202303039.
(41) Li, Q.; Ma, S.; Lu, N.; Qiu, J.; Ye, J.; Liu, Y.; Wang, S.; Han, Y.; Wang, B.; Xu, X.; Feng, H.; Zhu, J. Concurrent Thiol–Ene Competitive Reactions Provide Reprocessable, Degradable and Creep-Resistant Dynamic–Permanent Hybrid Covalent Networks. *Green Chem.* **2020**, *22* (22), 7769–7777. https://doi.org/10.1039/D0GC02823A.
(42) Van Herck, N.; Maes, D.; Unal, K.; Guerre, M.; Winne, J. M.; Du Prez, F. E. Covalent Adaptable Networks with Tunable Exchange Rates Based on Reversible Thiol–Yne Cross-Linking. *Angew. Chem. Int. Ed.* **2020**, *59* (9), 3609–3617. https://doi.org/10.1002/anie.201912902.
(43) Sendijarevic, V.; Sendijarevic, A.; Lekovic, H.; Lekovic, H.; Frisch, K. C. Polyoxazolidones for High Temperature Applications. *Journal of Elastomers & Plastics* **1996**, *28* (1), 63–83. https://doi.org/10.1177/009524439602800104.
(44) Sendijarevic, V.; Sendijarevic, A.; Frisch, K. C.; Reulen, P. Novel Isocyanate-Based Matrix Resins for High Temperature Composite Applications. *Polym. Compos.* **1996**, *17* (2), 180–186. https://doi.org/10.1002/pc.10603.

(45) Pankratov, V. A.; Frenkel', T. M.; Fainleib, A. M. 2-Oxazolidinones. *Russ. Chem. Rev.* **1983**, *52* (6), 576–593. https://doi.org/10.1070/RC1983v052n06ABEH002864.
(46) Gennen, S.; Grignard, B.; Tassaing, T.; Jérôme, C.; Detrembleur, C. CO_2-Sourced α-Alkylidene Cyclic Carbonates: A Step Forward in the Quest for Functional Regioregular Poly(Urethane)s and Poly(Carbonate)s. *Angew. Chem. Int. Ed.* **2017**, *56* (35), 10394–10398. https://doi.org/10.1002/anie.201704467.
(47) Ngassam Tounzoua, C.; Grignard, B.; Detrembleur, C. Exovinylene Cyclic Carbonates: Multifaceted CO $_2$ -Based Building Blocks for Modern Chemistry and Polymer Science. *Angew Chem Int Ed* **2022**, *61* (22). https://doi.org/10.1002/anie.202116066.
(48) Habets, T.; Siragusa, F.; Grignard, B.; Detrembleur, C. Advancing the Synthesis of Isocyanate-Free Poly(Oxazolidones)s: Scope and Limitations. *Macromolecules* **2020**, *53* (15), 6396–6408. https://doi.org/10.1021/acs.macromol.0c01231.
(49) Habets, T.; Siragusa, F.; Müller, A. J.; Grossman, Q.; Ruffoni, D.; Grignard, B.; Detrembleur, C. Facile Construction of Functional Poly(Monothiocarbonate) Copolymers under Mild Operating Conditions. *Polym. Chem.* **2022**, *13* (21), 3076–3090. https://doi.org/10.1039/D2PY00307D.
(50) Wong, A. R.; Barrera, M.; Pal, A.; Lamb, J. R. Improved Characterization of Polyoxazolidinones by Incorporating Solubilizing Side Chains. *Macromolecules* **2022**, *55* (24), 11006–11012. https://doi.org/10.1021/acs.macromol.2c02104.
(51) Sutherland, B. P.; Kabra, M.; Kloxin, C. J. Expanding the Thiol–X Toolbox: Photoinitiation and Materials Application of the Acid-Catalyzed Thiol–Ene (ACT) Reaction. *Polym. Chem.* **2021**, *12* (10), 1562–1570. https://doi.org/10.1039/D0PY01593H.
(52) Francis, T.; Thorne, M. P. Carbamates and 2-Oxazolidinones from Tertiary Alcohols and Isocyanates. *Can. J. Chem.* **1976**, *54* (1), 24–30. https://doi.org/10.1139/v76-006.
(53) Laurence, C.; Gal, J.-F. *Lewis Basicity and Affinity Scales: Data and Measurement*; John Wiley: Chichester, West Sussex, U.K, 2010.
(54) Pandit, N.; Singla, R. K.; Shrivastava, B. Current Updates on Oxazolidinone and Its Significance. *International Journal of Medicinal Chemistry* **2012**, *2012*, 1–24. https://doi.org/10.1155/2012/159285.
(55) Pulla, S.; Felton, C. M.; Ramidi, P.; Gartia, Y.; Ali, N.; Nasini, U. B.; Ghosh, A. Advancements in Oxazolidinone Synthesis Utilizing Carbon Dioxide as a C1 Source. *Journal of CO2 Utilization* **2013**, *2*, 49–57. https://doi.org/10.1016/j.jcou.2013.07.005.
(56) Sun, F.; Van Der Eycken, E. V.; Feng, H. Recent Advances in the Synthesis and Ring-Opening Transformations of 2-Oxazolidinones. *Adv. Synth. Catal.* **2021**, *363* (23), 5168–5195. https://doi.org/10.1002/adsc.202100746.
(57) Barbachyn, M. R.; Ford, C. W. Oxazolidinone Structure–Activity Relationships Leading to Linezolid. *Angew. Chem. Int. Ed.* **2003**, *42* (18), 2010–2023. https://doi.org/10.1002/anie.200200528.
(58) Denissen, W.; Rivero, G.; Nicolaÿ, R.; Leibler, L.; Winne, J. M.; Du Prez, F. E. Vinylogous Urethane Vitrimers. *Adv. Funct. Mater.* **2015**, *25* (16), 2451–2457. https://doi.org/10.1002/adfm.201404553.
(59) Lin, S.-K. Handbook of Polymers. By George Wypych, ChemTec Publishing, 2012; 680 Pages. Price $395.00, ISBN 978-1-895198-47-8. *Polymers* **2013**, *5* (1), 225–233. https://doi.org/10.3390/polym5010225.
(60) Ashby, M. F. *Materials Selection in Mechanical Design*, 2nd ed.; Butterworth-Heinemann: Oxford, OX ; Boston, MA, 1999.
(61) Lagron, A. B.; El-Zaatari, B. M.; Hamachi, L. S. Characterization Techniques to Assess Recyclability in Dynamic Polymer Networks. *Front. Mater.* **2022**, *9*, 915296. https://doi.org/10.3389/fmats.2022.915296.

(62) Van Lijsebetten, F.; De Bruycker, K.; Van Ruymbeke, E.; Winne, J. M.; Du Prez, F. E. Characterising Different Molecular Landscapes in Dynamic Covalent Networks. *Chem. Sci.* **2022**, *13* (43), 12865–12875. https://doi.org/10.1039/D2SC05528G.
(63) Maes, S.; Van Lijsebetten, F.; Winne, J. M.; Du Prez, F. E. *N* -Sulfonyl Urethanes to Design Polyurethane Networks with Temperature-Controlled Dynamicity. *Macromolecules* **2023**, *56* (5), 1934–1944. https://doi.org/10.1021/acs.macromol.2c02456.
(64) Schoustra, S. K.; Groeneveld, T.; Smulders, M. M. J. The Effect of Polarity on the Molecular Exchange Dynamics in Imine-Based Covalent Adaptable Networks. *Polym. Chem.* **2021**, *12* (11), 1635–1642. https://doi.org/10.1039/D0PY01555E.
(65) El-Zaatari, B. M.; Ishibashi, J. S. A.; Kalow, J. A. Cross-Linker Control of Vitrimer Flow. *Polym. Chem.* **2020**, *11* (33), 5339–5345. https://doi.org/10.1039/D0PY00233J.
(66) Spiesschaert, Y.; Taplan, C.; Stricker, L.; Guerre, M.; Winne, J. M.; Du Prez, F. E. Influence of the Polymer Matrix on the Viscoelastic Behaviour of Vitrimers. *Polym. Chem.* **2020**, *11* (33), 5377–5385. https://doi.org/10.1039/D0PY00114G.
(67) Swartz, J. L.; Sheppard, D. T.; Haugstad, G.; Dichtel, W. R. Blending Polyurethane Thermosets Using Dynamic Urethane Exchange. *Macromolecules* **2021**, *54* (23), 11126–11133. https://doi.org/10.1021/acs.macromol.1c01910.
(68) Chen, Z.; Sun, Y.-C.; Wang, J.; Qi, H. J.; Wang, T.; Naguib, H. E. Flexible, Reconfigurable, and Self-Healing TPU/Vitrimer Polymer Blend with Copolymerization Triggered by Bond Exchange Reaction. *ACS Appl. Mater. Interfaces* **2020**, *12* (7), 8740–8750. https://doi.org/10.1021/acsami.9b21411.
(69) Christensen, P. R.; Scheuermann, A. M.; Loeffler, K. E.; Helms, B. A. Closed-Loop Recycling of Plastics Enabled by Dynamic Covalent Diketoenamine Bonds. *Nat. Chem.* **2019**, *11* (5), 442–448. https://doi.org/10.1038/s41557-019-0249-2.
(70) Li, Q.; Ma, S.; Wang, S.; Yuan, W.; Xu, X.; Wang, B.; Huang, K.; Zhu, J. Facile Catalyst-Free Synthesis, Exchanging, and Hydrolysis of an Acetal Motif for Dynamic Covalent Networks. *J. Mater. Chem. A* **2019**, *7* (30), 18039–18049. https://doi.org/10.1039/C9TA04073K.
(71) Schenk, V.; Labastie, K.; Destarac, M.; Olivier, P.; Guerre, M. Vitrimer Composites: Current Status and Future Challenges. *Mater. Adv.* **2022**, *3* (22), 8012–8029. https://doi.org/10.1039/D2MA00654E.